



# Evaluation of Physico-Chemical Quality of Groundwater of Khemis Miliana Plain (North West Algeria)

Sadeuk Ben Abbas Abdelkader, Meddi Mohamed<sup>1</sup> and Boucefiane Abdelkader

University Djillali Bounama of Khemis Miliana, Algeria

<sup>1</sup>Higher National School of Hydraulic-Blida, Algeria

E-mail: [a.sadekbenabbes@univ-dbkm.dz](mailto:a.sadekbenabbes@univ-dbkm.dz)

**Abstract:** The demonstration of the main phenomena and the predominant chemical reactions in this evolution as well as the qualitative estimation of this water plus the comparison with the norms of the World Health Organization (W.H.O.), indicated that the positive (+) and negative (-) ions have a direct relationship with the geological and hydrogeological characteristics of the region. The maps of variation of hydro-chemical parameters were made for the spatial distribution of chemical components of groundwater, and also the Piper and Schoeller diagrams were used to know the chemical facies of waters. The groundwater chemistry of the study area shows that the most dominant facies is chloride-calcic in the north and chloride-sodium in the south of the plain. Diffuse pollution, more difficult to identify, which have an agricultural origin affect almost the entire plain according to the concentrations observed in all periods, especially in 2018 with a value of 107 mg / l in the East of the plain, where there is no agricultural activity.

**Keywords:** Quality, Physico-chemical, Groundwater, Plain of Khemis Miliana, Algeria

Water is an essential element for life and is important for countless human activities. Water may be scarce in some places, such as arid and semi-arid areas, or simply of poor quality in other places. It is certain that the increasing demand for water for human activities will increase the stress on this resource. In addition, natural factors, such as drought or geological constraints, have an effect on the supply and distribution of drinking water (Germain et al 2007). In its dynamics of development, Algeria did not address the issue relevant to hydrogeology and hydraulics all the intention which it deserves. This resulted in the disappearance of certain traditional orchards, the frequent tensions on water between cities and industries, a very significant decrease of the irrigated surface and the degradation of the quality of the underground water. It is therefore essential to quantify and analyse the quantity and quality of water reserves and to find ways of managing this resource to ensure its sustainability. In this context, the present study adds to earlier research works to provide a scientific overview of the current state of the Khemis Miliana region, from a qualitative and quantitative point of view (Abdelbak Boukli 2007, Caliano et al 2017, Kouadri et al 2021). The quality of the water in this region has deteriorated in recent years due to uncontrolled urban discharges, the intensive use of chemical fertilisers in agriculture, and disorderly exploitation. These elements change the chemistry of the water and make it unsuitable for desired uses (Bisht and Chauhan 2020). The study region has experienced, during the last years, a certain economic

and particularly agricultural expansion, and this after the application of the National Agricultural Development Program (PNDA) in 2000 and the National Fund for the Regulation of Agricultural Development (FNRDA) in 2002, this has on the one hand increased the demand for water and on the other hand, exploded the water resources to different pollutions resulting from the agricultural activity.

## MATERIAL AND METHODS

**Geographical location of the study area:** The study area is the plain of Khemis-Miliana. It is located 120 km south-west of Algiers, 50 km west of Médéa and 920 km east of Chlef, on the RN4 (Fig. 1) and altitude varies from 230 to 380 m. It is limited to the North by the western continuity of the djebel Zaccar (1578 m of altitude), to the South by the foothills of the Ouarsenis which culminates more than 200 m near Bordj-Bounama, to the East by djebel Gantas and to the West by the djebel Doui mountain. The surface area of the alluvial plain of Khemis Miliana is 360 km<sup>2</sup> and length is approximately 50 km for a width of 10 to 20 km.

The plain of Khemis Miliana is a vast area of depression with an East-West axis where Miocene, Pliocene and Quaternary sediments have accumulated (Fig. 2). The stratigraphy of the formations from bottom to top is as follows. The Primary consists of alternating layers of black shales and quartzites and clays. It is surmounted by the Triassic, which is generally made up of dolomites and dolomitic limestones, exposed in the Doui and Zaccar massifs). The Jurassic in the

Zaccar Massif is formed of compact, fractured and karstified limestones, overlain by sandstone shales and calcareous marls. The whole series reaches a thickness of about 700 m. At Jebel Doui, the Jurassic is mainly represented by dolomitic limestones with a thickness of about 80 m (Abbouda et al 2019). The Cretaceous is exposed on the lateral edges of the plain. It is represented by schist clays, about 800 m thick in the north and west of Zaccar and marls with interbedded limestone in the Dahra massif. The Miocene is up to 300 m thick. The lower Miocene is discordant on the ante-neogene basement and begins with a series of conglomerates about

220 m thick, then it ends with a marly series. The Miocene is marked by a new and progressive transgression. It begins with a series of blue marls visible mainly in the north-east of the plain, interspersed with clays and small sandy beds (Yelles et al 2009, Yahiaoui et al 2015). Fairly coarse red sandstones and interbedded conglomerates appear quite frequently in the Gantas and complete the Miocene cycle. The Mio-Pliocene consists of quartz pebbles, conglomerates, detrital sandstones and clays, and travertine deposited at the Zaccar sources.

**Hydrogeology**

**Main aquifers in the study area:** According to the study of the stratigraphic series and its lithological and structural characteristics, the following aquifer levels can be distinguished:

**Jurassic limestones:** Constitute an important reservoir which is characterised by the presence of fissures which favour the circulation and storage of water

**Miocene aquifers:** These are represented in the form of conglomerates of varying degrees of clay and sand.

**Pliocene aquifers:** Pliocene is in the form of Astian sandstones; with an average thickness of 100 m.

**Quaternary alluvial aquifers:** Quaternary alluvial formations constitute the most important and most exploited aquifer in the whole Khemis Miliana plain. The lithological descriptions of the boreholes show that more than 20% of the materials crossed are sands and gravels or sandstones and a range of borehole depths from 2 to 150 m.

**Inventory of water points:** Thirty six (36) water points were inventoried by the ANRH of El Khemis (Table 1) are

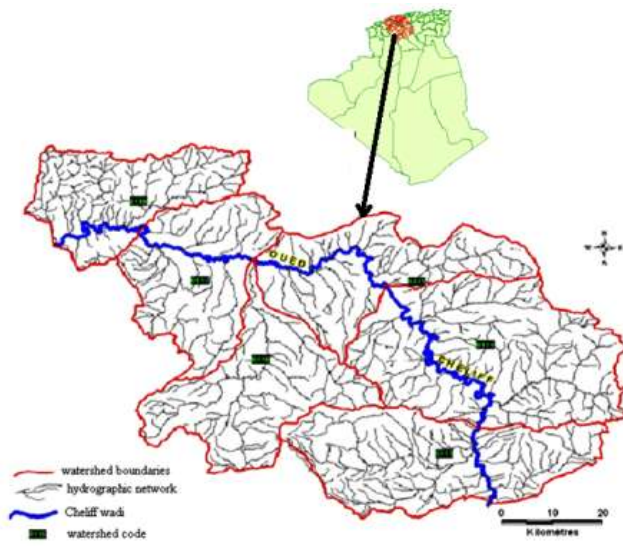


Fig. 1. Geographical location of the study area

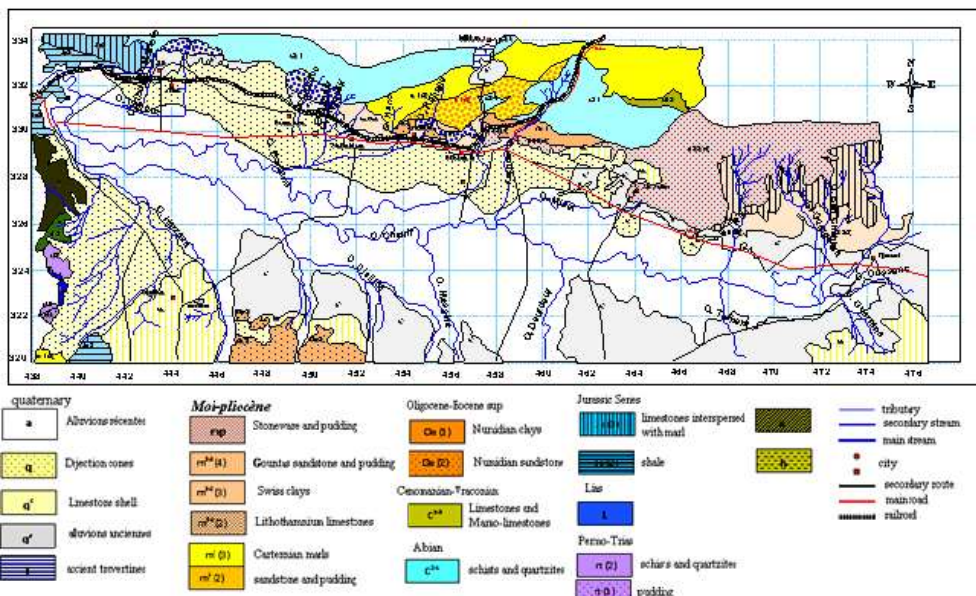


Fig. 2. Geological map of the Khemis Miliana plain (Geological map of Milian N°84)

**Table 1.** Inventory of water points (ANRH Khemis Miliana) based on the results of the well and borehole monitoring network

Water points	Coordinates		Z (m)	Depth
	X (m)	Y (m)		
84-5	461250	323550	287,41	15,69
84-8	462300	322800	293,40	20,66
84-12	462450	321750	308,38	21,21
84-14	462470	320850	315,80	25,10
84-39	461500	328000	292,83	23,11
84-57	456425	324400	275,73	13,92
84-63	452070	321950	280,60	15,00
84-72	454400	328400	279,30	12,59
84-73	453050	328950	277,30	8,50
84-80	448900	325250	260,12	17,00
84-91	447500	329600	256,64	5,50
84-92	447450	330600	284,31	21,10
84-93	449200	330800	286,90	32,41
84-107	447250	331000	264,81	17,00
84-110	441000	330100	246,76	12,00
84-114	446250	325250	264,53	15,00
84-125	442700	326000	258,29	20,00
84-127	441050	326350	274,14	16,00
84-129	440750	327900	251,75	8,65
84-136	459100	321900	295,92	17,90
84-139	459500	320900	303,64	15,00
84-140	458500	321300	296,90	11,20
84-143	458750	320300	301,10	14,00
84-154	456400	321850	290,05	16,20
84-155	456000	321050	293,02	13,50
84-166	442400	325250	269,18	12,72
84-169	442050	322650	313,15	12,01
84-182	444300	327550	252,28	16,00
84-185	457050	325500	274,84	8,21
84-196	447500	332600	278,02	13,01
84-310	456300	322100	289,75	19,10
84-311	455950	320250	310,84	18,00
84-313	443850	329500	250,85	23,00
84-314	454550	328350	279,22	280,00
85-6	471700	324700	346,26	18,00
85-14	469820	321500	316,43	19,50

distributed throughout the groundwater of Khemis Miliana for domestic and agricultural use, were subject to static level measurements, were used to establish piezometric maps (Fig. 3).

**Piezometry:** Piezometric maps, drawn up with data on piezometric levels, represent the spatial distribution of hydraulic loads and potentials at a given date. They also show the hydrodynamic boundary conditions. These maps will allow to determine the directions of groundwater flow, the recharge areas and the outlet of the water table. According to the piezometric maps of 2015 (Fig. 4a) and 2016 (Fig. 4b), flow directions converge towards Oued Cheliff where the water table feeds Oued Cheliff. However, the hydraulic gradient is quite strong in the eastern part and oscillates between  $8.33 \cdot 10^{-3}$  and  $7.14 \cdot 10^{-3}$  and in the south-western zone the hydraulic gradient becomes very strong and oscillates between  $1.66 \cdot 10^{-2}$  -  $1.25 \cdot 10^{-2}$ , on the other hand in the central and north-western part the hydraulic gradient is  $1.78 \cdot 10^{-3}$ . The piezometric maps of 2017 (Fig. 4d) and 2018 (Fig. 4c) show that the flow directions converge towards the Oued Cheliff where the water table feeds the latter with a drainage axis oriented from East to West. However, at the level of the city of Djendel and Djellida, the piezometric curves become narrower which implies a strong hydraulic gradient varying between  $8.33 \cdot 10^{-3}$  -  $1 \cdot 10^{-2}$ , and the city of Ain Sultan and the Doui Threshold, the piezometric curves become farther away which indicates a weak hydraulic gradient oscillating from  $2.5 \cdot 10^{-3}$  -  $1.22 \cdot 10^{-3}$ . During the low water period of 2015, a depression zone was observed in the central and north-western part of the plain; this is due to the intensive exploitation of the water table, particularly at the level of the overexploited boreholes "84-185, 84-92", and in 2018 a convergence of the groundwater in the central eastern and central western part of the plain was observed at the level of the overexploited boreholes "84-182, 84-8".

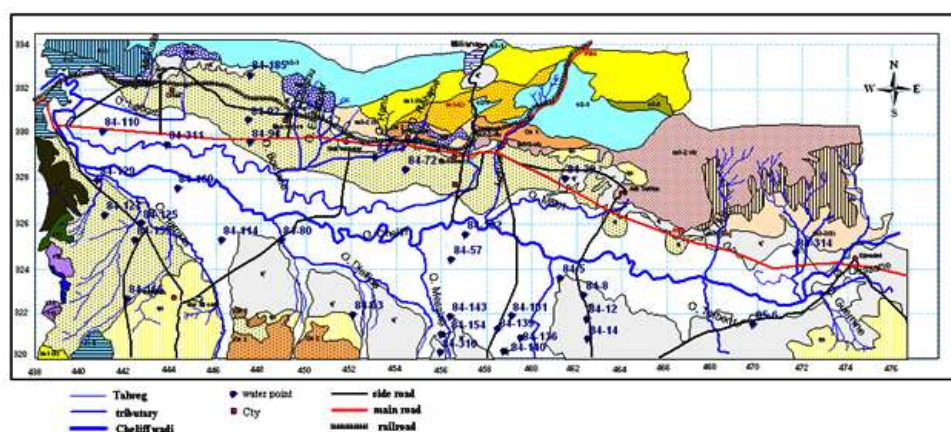


**Fig. 3.** Water point inventory map

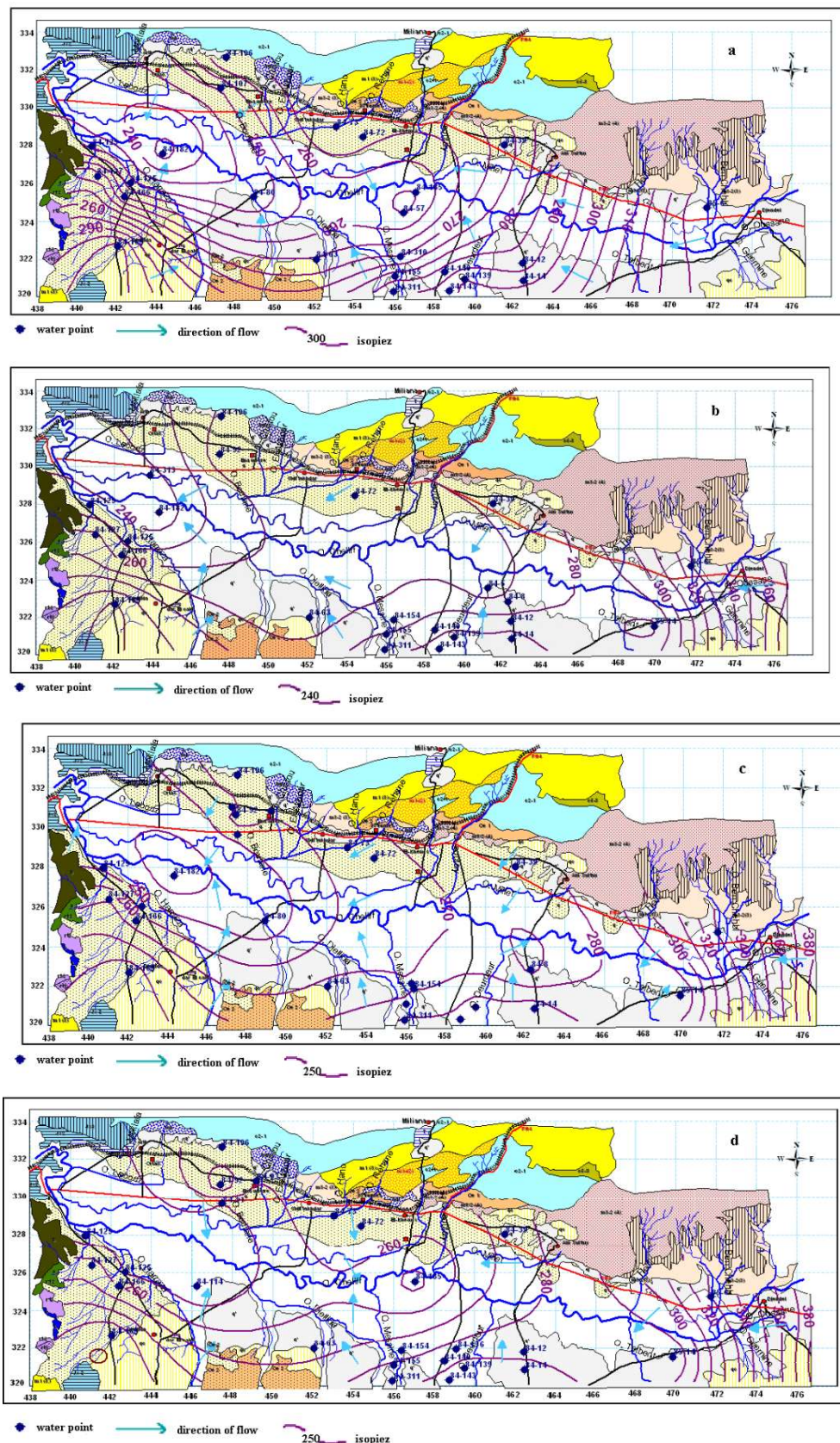


Fig. 4. Piezometric maps for 2015 (a), 2016 (b), 2017 (c), and 2018 (d)

**Physico-chemical parameters:** Water samples were taken in clean containers, rinsed several times with the water to be analysed, and closed tightly without leaving air bubbles in the bottle. They are kept in a at2-4°C until the time of analysis. Analyses were performed as soon as possible, but no later than 72 hours after the sample is taken. If this time cannot be met, it was necessary to prepare the samples for storage. For cations, the sample is filtered on a 0.45 µm filter (it is possible to use the filtration system for bacteriological analyses), then acidified with Hcl or NH3 to obtain a pH<2. For anions. there was no major problem of conservation. Samples prepared in this way can be stored for six months. Temperature, pH, conductivity, alkalinity and dissolved oxygen are measured in situ. These parameters are very sensitive to environmental conditions and are likely to change significantly if they are not measured on site. The total hardness of water was estimated as sum of Ca++ and Mg++ cations expressed in °F.

$$TH = [Ca^{++}] + [Mg^{++}] \dots \dots \dots (1)$$

Ca<sup>++</sup>, Mg<sup>++</sup> expressed in meq/l.

**Calculation of reaction quantity in meq/l:**

The meq/l was calculated as the ratio of the quantity of the element in reaction multiplied by the valency of the element divided by the molar mass of the same element

$$r = \frac{m \times \text{valence}}{M} (2)$$

r: the quantity in reaction in meq/l , m: the quantity in reaction in mg/l, M: the molar mass in g/mol

Quantity in reaction in relation to the sum of ions of the

same sign is calculated from the following formula:

$$r_c \% = \frac{r \times 100}{\sum r e^+} (3)$$

$$r_a \% = \frac{r \times 100}{\sum r e^-} (4)$$

rc%: reacting amount of cations, a%: reaction amount of anions: sum of cations and anions in meq/l

∑rc+: sum of cations in meq/l, ∑ra-: sum of anions in meq/l

**RESULTS AND DISCUSSION**

The average pH was 7.7 in 2015, the maximum is 8.3 and the minimum 7. In 2016, 2017 and 2018 the pH varied from 7.1 to 8.3 which indicates that the groundwater in the region is slightly alkaline

**Conductivity:** The conductivity values (Table 3) indicate a very high mineralization as they are globally higher than 1000 µs /cm. Most of the conductivities exceed 2 to 3 mS/cm. this salinity is primarily of geological origin (primary salinity). However, it tends to increase as a result of poor exploitation of boreholes, and can even be aggravated by anthropogenic pollution, making the water unsuitable even for irrigation (Achour et al 2008).

To study the chemical facies of the groundwater of the Khemis Miliana plain, projected the chemism of the sampled water points onto the Piper diagram (Fig. 5) and the Schoeller diagram (Fig. 6). Diagram software of the LHA (Simler et al 2012).

**Stabler's method:** The classification of waters consists of

**Table 2.** Analysis of the low water campaign 2015

Parameters	084-129	084-166	084-115	084-8	084-155	084-14	084-39	084-63	084-80	084-91	084-92	084-169	084-196	084-63
Ca <sup>2+</sup> (mg/l)	167	131	320	196	247	218	218	262	218	89	148	148	144	274
Mg <sup>2+</sup> mg/l	65	46	349	96	135	44	70	170	175	22	67	44	56	138
Na <sup>+</sup> mg/l	109	114	540	215	800	120	119	276	393	18	66	295	73	269
K <sup>+</sup> mg/l	17	2	4	4	6	4	2	4	7	15	2	0	0	19
Cl <sup>-</sup> mg/l	270	226	1 690	503	1 390	375	470	833	925	60	238	350	200	708
So <sub>4</sub> <sup>2-</sup> mg/l	237	110	570	267	458	138	149	438	583	166	190	320	187	600
Co3 mg/l	281	281	378	235	265	209	195	307	271	183	278	268	352	363
No <sub>3</sub> mg/l	78,0	56,0	1,0	82,0	46,0	73,0	26,0	33,0	17,0	3,0	62,0	48,0	17,0	33,0
r Ca <sup>2+</sup> %	2,33	2,24	1,32	1,92	1,04	2,83	2,67	1,84	1,38	3,09	2,62	1,52	2,64	1,96
r Mg <sup>2+</sup> %	1,50	1,29	2,37	1,55	0,94	0,93	1,41	1,97	1,81	1,27	1,94	0,75	1,67	1,62
r Na <sup>+</sup> %	1,32	1,69	1,94	1,83	2,93	1,35	1,27	1,69	2,16	0,55	1,02	2,63	1,16	1,67
r K <sup>+</sup> %	0,12	0,02	0,01	0,02	0,01	0,03	0,01	0,01	0,02	0,26	0,02	0,00	0,00	0,07
r Cl <sup>-</sup> %	0,88	0,95	1,81	1,30	1,82	1,33	1,58	1,46	1,45	0,41	0,87	1,00	0,75	1,17
r So <sub>4</sub> <sup>2-</sup> %	1,14	0,68	0,90	1,02	0,88	0,72	0,74	1,13	1,35	1,68	1,03	1,35	1,03	1,47
r HCo3%	1,57	2,02	0,69	1,05	0,59	1,27	1,12	0,92	0,73	2,15	1,75	1,32	2,25	1,03
r No3%	0,90	0,83	0,00	0,75	0,21	0,92	0,31	0,21	0,09	0,07	0,81	0,49	0,22	0,19

comparing the reaction qualities of cations and anions expressed as a percentage of the total concentration of the water using the characteristic Stabler formula (Table 4) and classifying the anions and cations separately in descending order to determine the chemical facies and the graphical representation of these elements on the diagram software (Simler 2009).

Piper, Schoeller Berkaloef and Stabler indicated that the dominant ions are most often chlorides among the anions and sodium among the cations. The most dominant chemical facies was the calcium chloride facies extending to the north-east and west of the plain, with a percentage of 53.5. Secondly, the sodium chloride facies with a percentage of 21.4 that develops in the south of the plain; this is probably due to the presence of recent fine-textured alluvium, the Magnesium-Chloride facies has a percentage of 14.3 and the last one is presented by the sodium-bicarbonate. The Stabler classification, based on reaction quantities, has proved useful as a complementary method to the Piper diagram. According to Jasmin and Mallikarjuna (2014), for the calcium chloride and magnesium sulphate family as well as for the

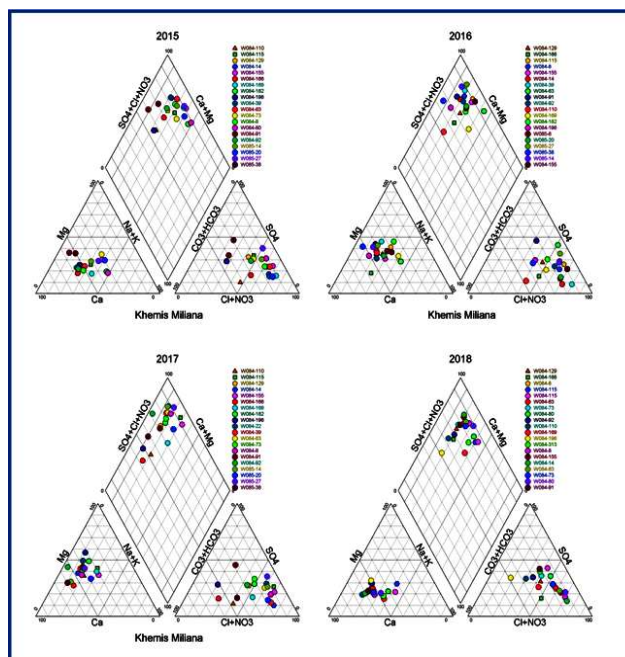


Fig. 5. Piper's diamond diagram of the groundwater of the Khemis Miliana plain

Table 3. Conductivity and pH values

Période	2015		2016		2017		2018	
	pH	CE $\mu\text{/cm}$	pH	CE $\mu\text{/cm}$	pH	CE $\mu\text{/cm}$	pH	CE $\mu\text{/cm}$
W084-110	7	1,034	7.8	1,600	8	4,000	7.9	1,800
W084-115	7.8	3,500	7.6	3,470	8.2	1,200	7.5	4,750
W084-129	7.8	1,702	7.8	5,210	8.1	2,490	7.3	4,080
W084-14	7.6	3,160	7.6	3,000	8	1,800	7.2	1,928
W084-155	7.5	5,260	7.7	3,500	8	4,460	7.8	3,880
W084-166	7.7	1,512	7.7	333	7.9	3,000	7.4	3,620
W084-169	7.4	3,130	7.9	3,800	7.4	5,000	7.3	2,580
W084-182	7.4	4,000	7.6	3,780	7.7	2,200	7.5	2,890
W084-196	7.6	1,292	8	4,080	7.4	2,000	7.7	2,400
W084-39	7.7	2,540	7.7	3,400	8	2,400	7.1	1,313
W084-63	7.6	3,600	7.8	1,224	8	3,900	7.7	3,650
W084-73	7.8	3,030	7.5	3,430	8	2,350	7.7	4,200
W084-8	7.5	2,670	7.6	5,310	7.8	2,300	7.8	2,350
W084-80	7.7	4,300	7.6	3,000	7.4	2,800	7.2	2,720
W084-91	7.6	7,35	7.5	2,850	7.3	4,700	7.3	3,420
W084-92	7.6	1,565	7.3	3,440	7.5	3,500	7.3	1,369
W085-14	7.9	4,000	7.9	2,970	8.1	2,980	7.3	3,450
W085-20	7.6	2,700	8.3	1,500	7.4	1,300	7.3	900
W085-27	7.5	5,840	8.1	6,100	7.5	3,800	7.3	4,060
W085-38	7.7	1,200	8.1	2,000	7.5	3,500	7.2	3,170
W085-6	7.5	2,510	7.8	1,653	7.5	1,500	8.3	2,720

sodium chloride and potassium family, the lithology of the aquifer is thinner, the circulation of water is difficult, the contact time between water and rock increases, hence the increase in salinity, and the influence of the clays becomes more marked. This interpretation reflects the phenomenon of concentration by dissolution.

#### Maps

**Calcium  $Ca^{2+}$ :** Figure 7 represents the evolution of  $Ca^{2+}$  in the plain of Khemis Miliana during the five and the values of  $Ca^{2+}$  vary between 49 and 466 mg/l, which exceed the WHO standards (200 mg/l). The highest  $Ca^{2+}$  were concentrated in the central part of the plain during the period of 2015, 2015, and 2017 which corresponds to the years of climatic and hydrological drought. The values that do not exceed the WHO standards correspond to the period of 2018, and from 2015 to 2018, the  $Ca^{2+}$  values started to increasing especially in the

southern edges of the plain. The exceedance of the  $Ca^{2+}$  concentration in the period 2015 is mainly due to the dissolution of limestone in this part or to the residence time. The decrease of this element in 2018 is due to the dilution of these waters by the inflow of water due to the high precipitation of this year or by the infiltration of water from the releases of the dams.

**Magnesium  $Mg^{2+}$ :** Figure 8 shows the evolution of  $Mg^{2+}$  over the five periods which varies between 18 and 320 mg/l.  $Mg^{2+}$  concentrations hardly exceed the WHO quality standards (150 mg/l) in 2016, however, for the periods 2015 a slight increase in concentration can be observed on the southern edges of a central part of the plain. This increase is perhaps due to the exchanges of the plain of Khemis Miliana with the wad's Massine, Djellida and Harrazza. The decrease of this concentration in the period of 2016 is probably due to the dilution by the heavy precipitations.

**Table 4.** Chemical facies classification according to Stabler

Water points	Classification	Chemical facies
84-129	$Ca^{2+} > Na^{+} > Mg^{2+} > K^{+} Cl^{-} > SO_4^{2-} > HCO_3^{-} > NO_3^{-}$	Chloride-Calcium
84-166	$Ca^{2+} > Na^{+} > Mg^{2+} Cl^{-} > HCO_3^{-} > SO_4^{2-} > NO_3^{-}$	Chloride-Calcium
84-115	$Mg^{2+} > Na^{+} > Ca^{2+} Cl^{-} > SO_4^{2-} > HCO_3^{-}$	Chloride-Magnesium
84-8	$Ca^{2+} > Na^{+} > Mg^{2+} Cl^{-} > SO_4^{2-} > HCO_3^{-} > NO_3^{-}$	Chloride-Calcium
84-155	$Na^{+} > Ca^{2+} > Mg^{2+} Cl^{-} > SO_4^{2-} > HCO_3^{-} > NO_3^{-}$	Chloride- Sodium
84-14	$Ca^{2+} > Na^{+} > Mg^{2+} > K^{+} Cl^{-} > HCO_3^{-} > SO_4^{2-} > NO_3^{-}$	Chloride-Calcium
84-39	$Ca^{2+} > Mg^{2+} > Na^{+} Cl^{-} > HCO_3^{-} > SO_4^{2-} > NO_3^{-}$	Chloride-Calcium
84-63	$Mg^{2+} > Ca^{2+} > Na^{+} Cl^{-} > SO_4^{2-} > HCO_3^{-} > NO_3^{-}$	Chloride-Magnesium
84-80	$Na^{+} > Mg^{2+} > Ca^{2+} Cl^{-} > SO_4^{2-} > HCO_3^{-} > NO_3^{-}$	Chloruré - Sodique
84-91	$Ca^{2+} > Mg^{2+} > Na^{+} > K^{+} SO_4^{2-} > HCO_3^{-} > Cl^{-} > NO_3^{-}$	Sulphate-Calcium
84-92	$Ca^{2+} > Mg^{2+} > Na^{+} Cl^{-} > HCO_3^{-} > SO_4^{2-} > NO_3^{-}$	Chloride-Calcium
84-169	$Na^{+} > Ca^{2+} > Mg^{2+} Cl^{-} > SO_4^{2-} > HCO_3^{-} > NO_3^{-}$	Chloruré-Sodique
84-196	$Ca^{2+} > Mg^{2+} > Na^{+} Cl^{-} > HCO_3^{-} > SO_4^{2-} > NO_3^{-}$	Bicarbonate-Calcium
84-63	$Ca^{2+} > Na^{+} > Mg^{2+} > K^{+} Cl^{-} > SO_4^{2-} > HCO_3^{-} > NO_3^{-}$	Chloride-Calcium
84-129	$Ca^{2+} > Mg^{2+} > Na^{+} > K^{+} Cl^{-} > SO_4^{2-} > HCO_3^{-} > NO_3^{-}$	Chloride-Calcium
84-166	$Ca^{2+} > Na^{+} > Mg^{2+} Cl^{-} > HCO_3^{-} > SO_4^{2-} > NO_3^{-}$	Chloride-Calcium
84-115	$Mg^{2+} > Na^{+} > Ca^{2+} Cl^{-} > SO_4^{2-} > HCO_3^{-}$	Chloride-Magnesium
84-8	$Ca^{2+} > Na^{+} > Mg^{2+} Cl^{-} > SO_4^{2-} > HCO_3^{-} > NO_3^{-}$	Chloruré- Calcique
84-155	$Na^{+} > Ca^{2+} > Mg^{2+} Cl^{-} > SO_4^{2-} > HCO_3^{-} > NO_3^{-}$	Chloruré-Sodique
84-14	$Ca^{2+} > Na^{+} > Mg^{2+} > K^{+} Cl^{-} > HCO_3^{-} > SO_4^{2-} > NO_3^{-}$	Chloride-Calcium
84-39	$Ca^{2+} > Mg^{2+} > Na^{+} Cl^{-} > HCO_3^{-} > SO_4^{2-} > NO_3^{-}$	Chloride-Calcium
84-63	$Mg^{2+} > Ca^{2+} > Na^{+} Cl^{-} > SO_4^{2-} > HCO_3^{-} > NO_3^{-}$	Chloride-Magnesium
84-80	$Na^{+} > Mg^{2+} > Ca^{2+} Cl^{-} > SO_4^{2-} > HCO_3^{-} > NO_3^{-}$	Chloruré-Sodique
84-91	$Ca^{2+} > Mg^{2+} > Na^{+} > K^{+} SO_4^{2-} > HCO_3^{-} > Cl^{-} > NO_3^{-}$	Sulphate-Calcium
84-92	$Ca^{2+} > Mg^{2+} > Na^{+} Cl^{-} > HCO_3^{-} > SO_4^{2-} > NO_3^{-}$	Chloride-Calcium
84-169	$Na^{+} > Ca^{2+} > Mg^{2+} Cl^{-} > SO_4^{2-} > HCO_3^{-} > NO_3^{-}$	Chloruré-Sodique
84-196	$Ca^{2+} > Mg^{2+} > Na^{+} HCO_3^{-} > Cl^{-} > SO_4^{2-} > NO_3^{-}$	Bicarbonate- Calcique
84-63	$Ca^{2+} > Na^{+} > Mg^{2+} > K^{+} Cl^{-} > SO_4^{2-} > HCO_3^{-} > NO_3^{-}$	Chloride-Calcium

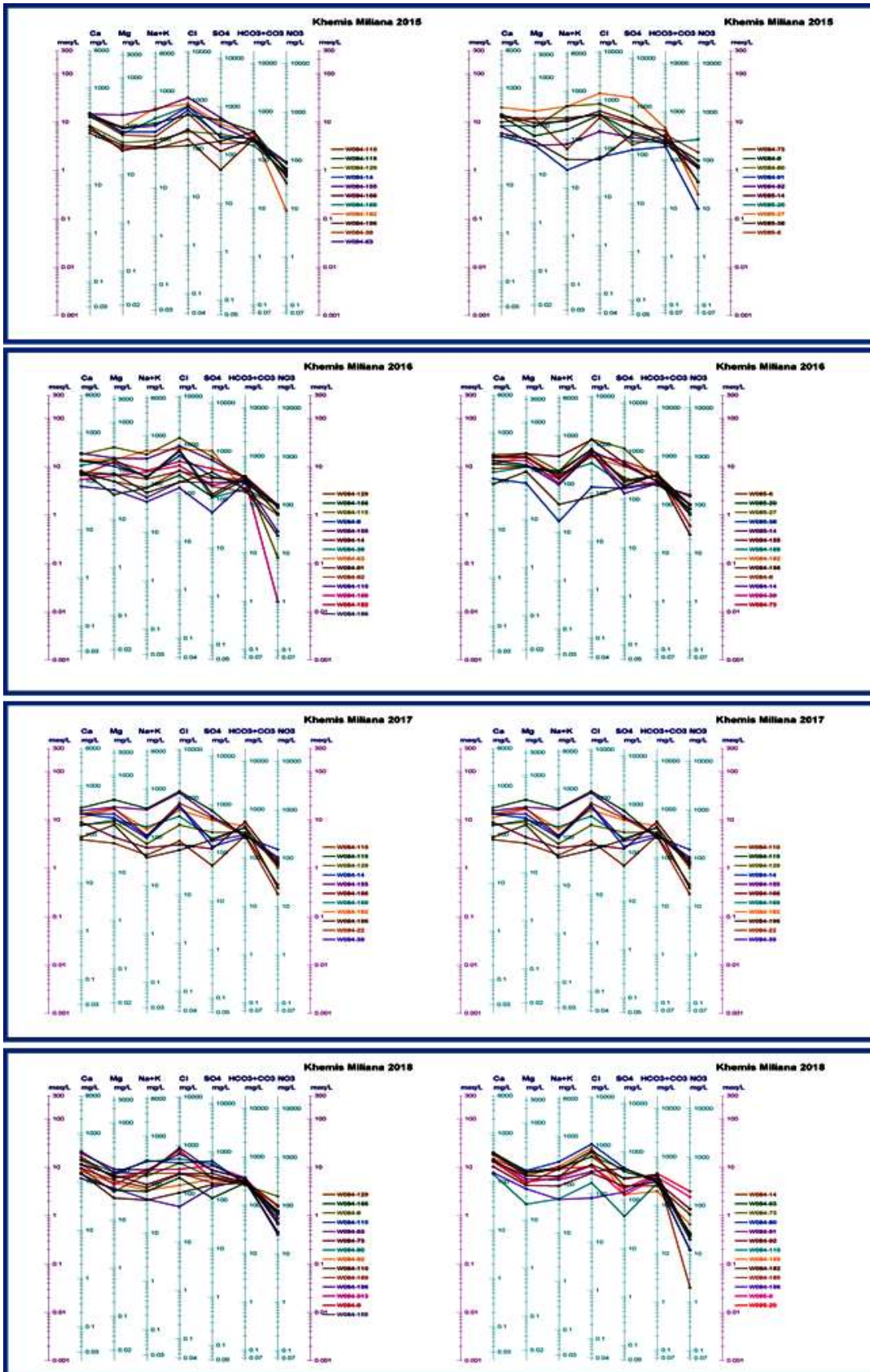


Fig. 6. Scholler logarithmic diagram for the groundwater of the Khemis Miliana plain



**Sodium Na<sup>+</sup>:** Figure 9 shows that the Na<sup>+</sup> values vary between 12 and 800 mg/l, which exceed the WHO drinking water standards of 200 mg/l. This increase is due to the evolution of this chemical element. This may be due to the leaching of rock salt. This increase is very remarkable in the southern and central part of the plain, due to the presence of a diapir in the Triassic formations.

**Potassium K<sup>+</sup>:** These values are relatively low, with concentrations ranging from 0 to 48 mg/l, which exceeds the WHO potability standards of 12 mg/l (Fig. 10). This increase may be due to the exchange of the Khemis Miliana plain with the tributaries.

**Chlorides Cl<sup>-</sup>:** According to figure 11, the contents of Cl<sup>-</sup> ranged between 55 and 1690 mg/l, which exceeds the standards of WHO (250 mg/l), strong concentration of Cl<sup>-</sup> is observed during 2015, 2016 and 2017 in the southern part of the plain and can be the result of the presence of rock salts (Na Cl, CaCl<sub>2</sub>) "Halite", or by the infiltration of water from the

wadis, and from the period of 2018 observed a decrease in this concentration which is possibly due to dilution by water inputs Except in the central part where the inhabitants of this

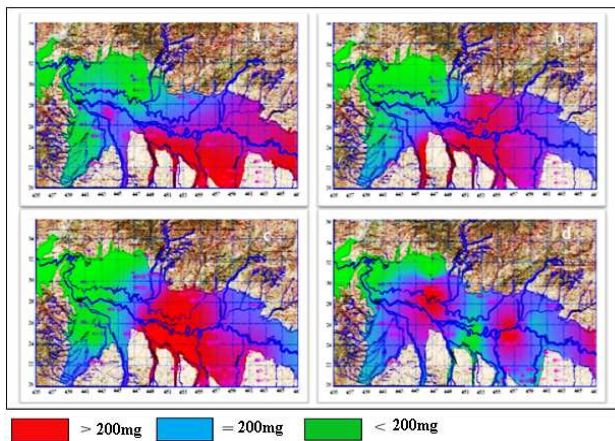


**Fig. 7.** Spatial variation of calcium levels in groundwater of the Hkemis Miliana plain (a: 2015, b: 2016, c: 2017, d: 2018)

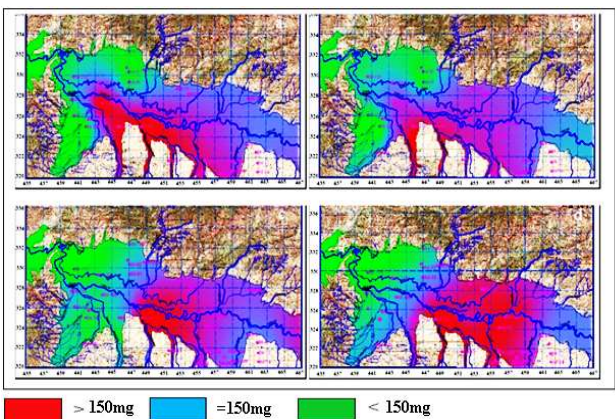


**Fig. 8.** Spatial variation of magnesium content in groundwater of the Hkemis Miliana plain (a: 2015, b: 2016, c: 2017, d: 2018)

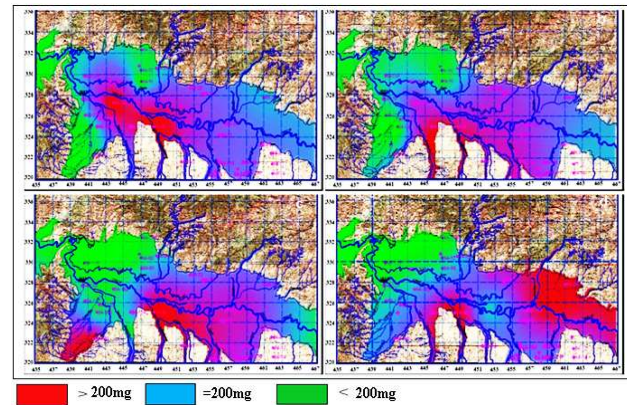


**Fig. 9.** Spatial variation of sodium levels in groundwater of the Hkemis Miliana plain (a: 2015, b: 2016, c: 2017, d: 2018)

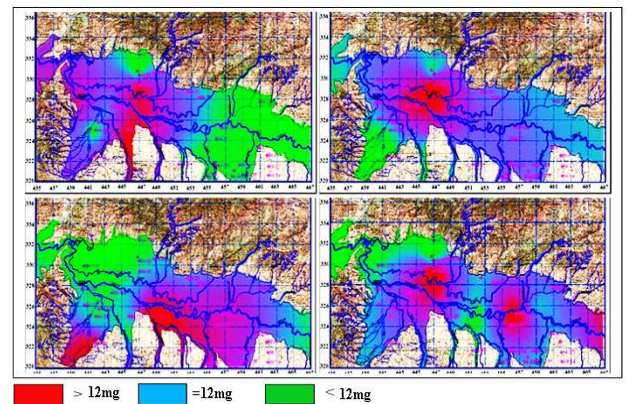


**Fig. 10.** Spatial variation of potassium levels in groundwater of the Hkemis Miliana plain (a: 2015, b: 2016, c: 2017, d: 2018)

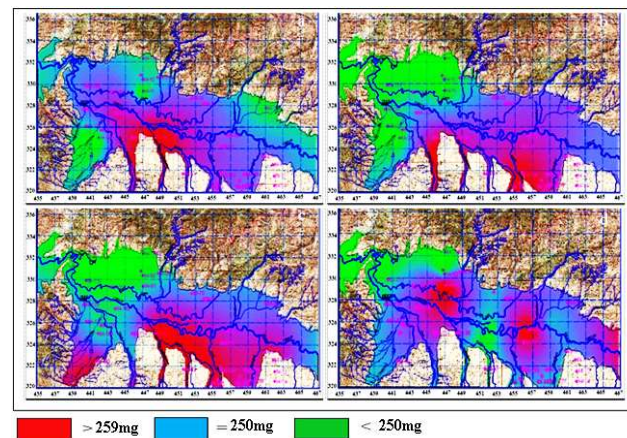


**Fig. 11.** Spatial variation of groundwater chloride levels in the Hkemis Miliana plain (a: 2015, b: 2016, c: 2017, d: 2018)

region are concentrated, which explains that the cause of this pollution is due to domestic discharges.

**Sulphates  $SO_4^{2-}$ :** The concentrations of  $SO_4^{2-}$  vary between 47 and 2185 mg/l which are above the WHO standard (250 mg/l) with high concentrations recorded at the southern edges and the central part of the plain in the 2015 (Fig. 12). In 2016 and 2017 the concentration increases sharply in the whole central part of the plain, this increase is possibly due to gypsum outcrops, note that gypsum is a hydrated sulphate ( $Ca SO_4 2H_2O$ ), either it is of agricultural origin or it is due to domestic and industrial discharges.

**Bicarbonates  $HCO_3^-$ :** The bicarbonate level in the waters of the Khemis Miliana plain varied between 153 and 763 mg/l which exceeds the WHO standards (400 mg/l). There was increase in the concentration during 2015, 2016 and 2017, decreased during 2018 (Figure 13). This phenomenon is explained in the same way as  $Ca^{2+}$ .

**Anthropogenic pollution:** Urban, agricultural and industrial development often leads to rapid pollution of groundwater by chemical forms of nitrogen, especially nitrate, due to their high solubility and low affinity to ion exchange. The other forms of nitrogen appear only under reducing conditions. In order to identify the problem of the evolution of this pollution of the groundwater of the Khemis Miliana plain, based on the comparison of nitrate concentrations for different periods superimposed it on the land use map to find out if there is a pollution of agricultural origin. Figure 15 shows the evolution of nitrate concentrations during the years 1993, 2002, 2003, 2008, 2009 and 2010.

Figure 15 shows that nitrates exceed the standards required by the WHO. The concentration reached up to 250 mg/l in 2009, and there is also a trend of a progressive evolution of the concentration over time. The selected water points do not capture the same aquifer, which makes the comparison very delicate to this effect the ANRH of Bilida realized a new monitoring network composed of 14 well-equipped piezometers capturing all the water table, we are lucky to have a series of analysis of this new network (Table 5).

Nitrates occur naturally in groundwater. A natural level exists but does not exceed a concentration of 10 mg/l. The maximum concentration authorized for public use is 50 mg/l. It is the "artificial" pollution that increases the nitrate levels and exceeds the norm. The plain of Khemis Miliana is confronted with major pollution problem and the threshold of 50 mg/l is often exceeded. The values are increasing, the groundwater is more and more loaded with nitrates but except for some delicate sectors, the 50 mg/l is still rarely reached. The two types of pollution were observed. Point source pollution, easy to locate, comes from industrial or

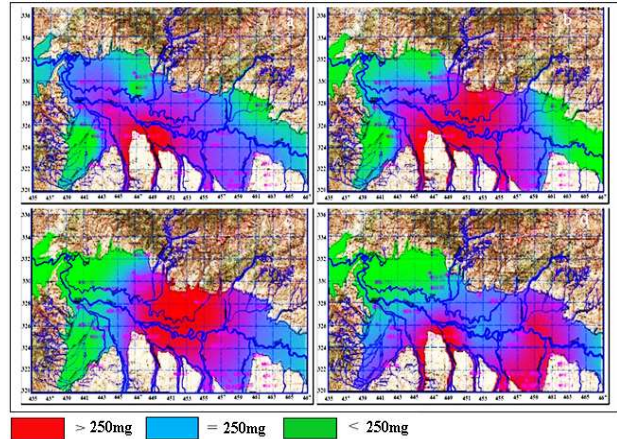


Fig. 12. Spatial variation of sulphate levels in the groundwater of the Hkemis Miliana plain (a: 2015, b: 2016, c: 2017, d: 2018)

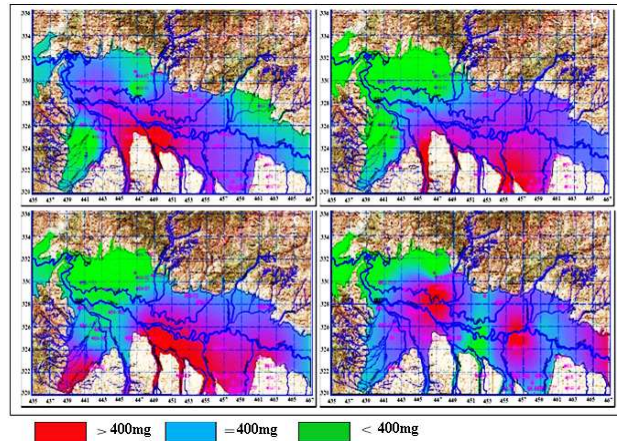


Fig. 13. Spatial variation of bicarbonate contents in the groundwater of the Hkemis Miliana plain (a: 2015, b: 2016, c: 2017, d: 2018)

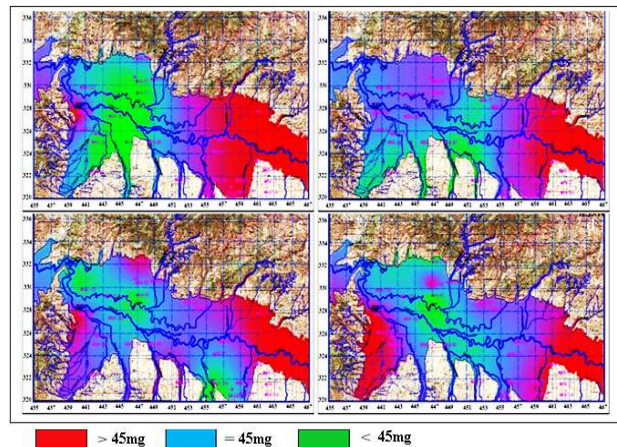


Fig. 14. Spatial variation of groundwater nitrate levels in the Hkemis Miliana plain (a: 2015, b: 2016, c: 2017, d: 2018)

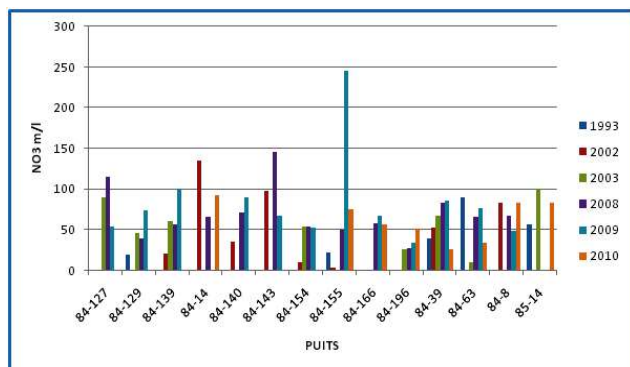


Fig. 15. Variation of nitrate for the periods (1993, 2002, 2003, 2008, 2009 and 2010)

domestic discharges, which are very noticeable in the western part of the plain, where the big cities are located (Khemis Miliana, Sidi Lakhdar, Arib and Ain Defla) as well as industrial activities such as the Aribes dairy, the Sidi Lakhdar sugar factory and the Ain Defla industrial zone. Diffuse pollution, more difficult to identify, has an agricultural origin, which affects almost the entire plain according to the concentrations observed in all periods, especially that of the year 2018 observed in the piezometer PZ1A with a value of 107 mg/l in the east of the plain, where there is no agricultural activity (Fig. 16). The carryover of soil constituents, in this case nitrates, depend on the one hand on climatic conditions, precipitation volume (drainage) and temperature

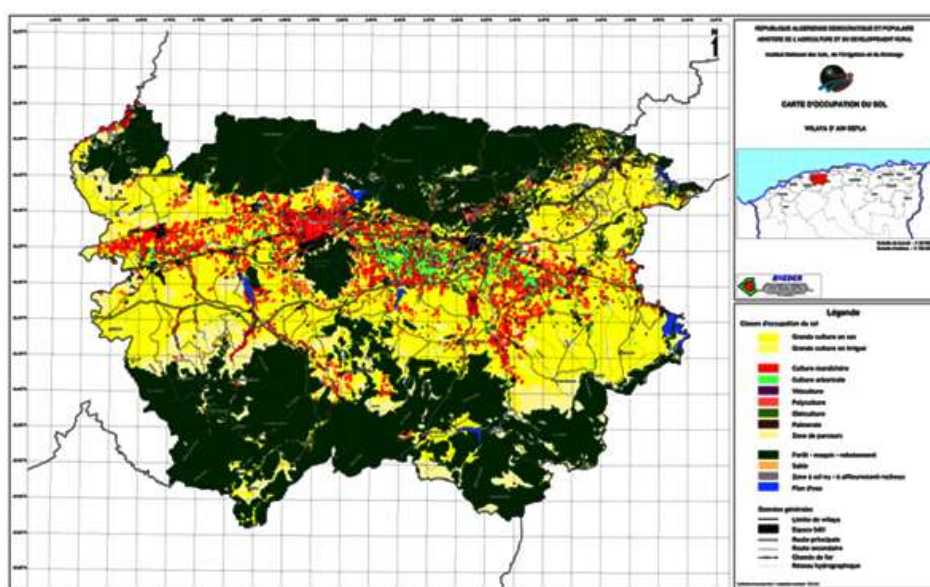


Fig. 16. Land use map of the study area (2011)

Table 5. Nitrate values at the Piezometers for the period 2014-2018

Wells	2014	2015	2016	2017	2018
PZ1A	37.0	8.0	8.0	5.0	107.0
PZ3A	37.0	35.0	35.0	5.0	3.0
PZ4A	23.0	34.0	34.0	4.0	9.0
PZ5A	33.0	17.0	17.0	5.0	0.0
PZ6A	0.0	3.0	3.0	47.0	7.0
PZ7A	1.0	0.0	0.0	5.0	0.5
PZ9A	2.0	0.0	0.0	7.0	0.5
PZ10A	23.0	4.0	4.0	6.0	0.5
PZ11A	1.0	4.0	4.0	0.0	0.5
PZ12A	1.0	0.0	0.0	1.0	0.5
PZ13A	2.0	2.0	2.0	0.0	6.0
PZ14A	6.0	7.0	7.0	13.0	0.5
PZ15A	-	4.0	4.0	1.0	22.0

(evaporation) and on the other hand on plant cover and biological activity. Not all surfaces are equal when it comes to nitrate carryover. Bare soil will react differently from cultivated soil. On ploughed land, the danger is after the harvest, at the end of summer and beginning of autumn, when the rains start again on a warm and aerated soil, a factor that favours the bacterial mineralization of humus, and the leaching of soil constituents towards the water table is very important. The land use map of the study area (Fig. 16) shows that agricultural activities are very intense, particularly market gardening, dry farming, irrigated farming and tree farming, where the farmer uses a large quantity of fertilizer and irrigation is provided from groundwater. There was a National Agricultural Development Programme (PNDA) in 2000 and a National Agricultural Development Regulation Fund (FNRDA) programme in 2002 which aggravated the situation because the authorities allowed water drilling in the plain for those who have at least ten hectares of cultivated land without respecting the boundary conditions or the protection perimeter of the plain.

#### CONCLUSION:

The lithostratigraphic and geological study determined the formations likely to be aquiferous which are presented by the multilayer aquifer with interstitial porosity formed by the Quaternary alluvium and the Mio-Pliocene sands and sandstones, and an aquifer composed by the Jurassic fissured limestone's. The hydrogeological study estimated that aquifer horizons represented by the Mio-Plio-Quaternary water table and that of the Jurassic limestones and this confirms the geological study. The evolution of the chemical facies since 2015 to 2018 with a dominance of the calcium chloride type in the North and sodium chloride type in the South of the plain. The maps of the variations of the various chemical elements have made it possible to determine the evolution of these parameters during four periods which present an excess of certain constituents, in particular Ca<sup>++</sup>, Na<sup>+</sup> and Cl<sup>-</sup> at the central southern edges of the plain. In addition, the highest concentrations of nitrates affecting the whole plain are explained by the important use of fertilizers which have harmful effects on the health of living beings.

Nitrate levels in the plain of Khemis Miliana show that the area near the agglomerations of Djendel, Bir Ouled Khelifa and Djelida is much more exposed to pollution, with levels exceeding 50 mg/l. These high nitrate levels can be explained by the presence of various sources of pollution linked mainly to agriculture, livestock farming and urban practices (domestic and industrial waste). The majority of the chemical elements analysed exceed the standards set by the WHO. Indeed, the high levels of calcium, sodium and

potassium make these waters very hard. For a more in-depth knowledge of the evolution of the quality of the groundwater of the Khemis Miliana plain, recommend that the general public be regularly made aware of the proper use of fertilisers in agricultural areas in order to reduce the contamination of the water table, particularly by nitrates, and that periodic checks be carried out on the quality of the groundwater. One or more monitoring points should be set up between the pollution zones and the water catchment area with the use of a geographic information system for qualitative and quantitative management of the water resource.

#### REFERENCES

- Abbouda M, Maouche S, Bouhadad Y and Belhai D 2019. Neotectonics and active tectonics of the Dahra-Lower Cheliff Basin (Tell Atlas, Algeria): Seismotectonic implication. *Journal of African Earth Sciences* **153**: 250-267.
- Abdelbaki Boukli C and Boukli HF 2007. Study of the groundwater degradation phenomenon of the urban grouping of Tlemcen. *Journal of Renewable Energies* **10**(2): 257-263.
- Achour S, Youcef L and Guergazi S 2008. Physico-chemical quality of groundwater and surface water in the Algerian Eastern Northern Sahara, Rev. **EIN311**: 79-84. (in French).
- Achour S, Tibermacine A and Chabbi F 2017. Iron and manganese in natural waters and chemical oxidation methods. Case of Algerian waters. *LARHYSS Journal* **32**: 139-154.
- Awad S 2011. Hydrochemistry and geochemical facies of groundwater, Bekaa Plain. *Hydrological Sciences Journal* **56**(2):
- Bisht N, Mishra SK and Chauhan PS 2020. Bacillus amyloliquefaciens inoculation alters physiology of rice (*Oryza sativa* L. var. IR-36) through modulating carbohydrate metabolism to mitigate stress induced by nutrient starvation. *International Journal of Biological Macromolecules* **143**: 937-951.
- Bouchemal F 2015. Physicochemical quality and pollution parameters of groundwater in the Biskra region. *Larhyss Journal*, **12**(2): 197-212. (in French).
- Calianno M, Reynard E, Milano M and Buchs A 2017. Quantifying water uses: A terminological and conceptual clarification to remove confusions. *Vertigo-the Electronic Journal in Environmental Sciences* **17**(1).
- El Hammoumi N, Sinan M, Lekhlif B and El Mahjoub L 2012. Assessment of groundwater quality for use in drinking water and agriculture: plain of Tadla, Morocco. *Afrique Science: International Journal of Science and Technology* **8**(1). (in French).
- Germain Kobenan N'guettia, Jules Mangoua Oi Mangoua, Narcisse Kouassi BOUA Jaouad El Asslouj, Sanae Kholtei, Namira El Amrani-Paaza and Abderrauf Hilali 2007 The impact of anthropogenic activities on the quality of groundwater in the Mzamza community (Chaouia, Morocco) *Journal of Water Science* **20**(3): 309-321.
- Ghesquière O, Walter J, Chesnaux R and Rouleau A 2015. Scenarios of groundwater chemical evolution in a region of the Canadian Shield based on multivariate statistical analysis. *Journal of Hydrology: Regional Studies* **4**: 246-266.
- Jaouad El Asslouj, Sanae Kholtei, Namira El Amrani-Paaza and Abderrauf Hilali 2007 The impact of anthropogenic activities on groundwater quality in the Mzamza community (Chaouia, Morocco) *Journal of Water Science* **20**: 309-321. (in French).
- Jasmin I and Mallikarjuna P 2014. Physicochemical quality evaluation of groundwater and development of drinking water quality index for Araniar River Basin, Tamil Nadu, India. *Environmental Monitoring and Assessment* **186**(2): 935-948.

- Kouadri S, Kateb S and Zegait R 2021. Spatial and temporal model for WQI prediction based on back-propagation neural network, application on EL MERK region (Algerian southeast). *Journal of the Saudi Society of Agricultural Sciences* **20**(5): 324-336.
- Simler R 2009. Diagrammes software. Downloadable at <http://www.lha.univ-avignon.fr/LHA-Logiciels.htm>
- Simler BR, Hui G, Dahl JE and Perez-Ramirez B 2012. Mechanistic complexity of subvisible particle formation: Links to protein aggregation are highly specific. *Journal of Pharmaceutical Sciences* **101**(11): 4140-4154. (in French).
- Yahiaoui I, Douaoui A, Zhang Q and Ziane A 2015. Soil salinity prediction in the Lower Cheliff plain (Algeria) based on remote sensing and topographic feature analysis. *Journal of Arid Land* **7**(6): 794-805.
- Yelles A, Domzig A, Déverchère J, Bracène R, de Lépinay BM, Strzeczynski P and Djellit H 2009. Plio-Quaternary reactivation of the Neogene margin off NW Algiers, Algeria: the Khayr al Din bank. *Tectonophysics* **475**(1): 98-116.

---

Received 28 January, 2022; Accepted 22 May, 2022